

Modeling of Boron Deactivation/Activation Kinetics During Ion Implant Annealing

Srinivasan Chakravarthi

Department of Manufacturing Engineering, Boston University, Boston, MA, 02215.
email: srini@bu.edu

Scott T. Dunham

Department of Electrical Engineering, University of Washington, Seattle, WA 98195.

Abstract— Boron Transient Enhanced Diffusion (TED) is characterized by enhanced tail diffusion coupled with an electrically inactive immobile peak associated with the clustering of boron in the presence of excess interstitials. A consistent model for process simulation has to account for the formation of a variety of agglomerates associated with the excess point defect concentrations following ion implantation. These include interstitial clusters (e.g., {311} defects), vacancy clusters and dopant/interstitial clusters (e.g., boron interstitial clusters). In addition to the chemical profiles (SIMS) it is essential to also predict electrical activation behavior. Hence, in this work we investigate models for boron deactivation and subsequent activation during annealing.

I. INTRODUCTION

It is well known that boron exhibits anomalous diffusion during the initial phase of annealing after ion implantation. B TED is characterized by an enhanced tail diffusion coupled with an electrically inactive immobile peak. The electrically inactive peak has now been widely accepted to be due to clustering of boron in the presence of excess interstitials. Although a number of research groups have published modeling of boron chemical profiles [1], [2], [3] little physical modeling has been published in regard to electrical activation. Since predicting electrical activation is essential to TCAD, in this work we look at modeling of boron electrical activation during transient enhanced diffusion.

II. MODEL

A consistent model for boron transient enhanced diffusion must consider the initial point defect recombination and the subsequent formation of extended defects associated with the remaining interstitial excess, such as {311} defects and boron interstitial clusters (BICs).

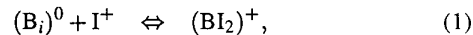
A. Initial Damage

Implantation introduces a large number of point defects orders of magnitude higher than the dopant concentration. However, these excess point defects quickly recombine and lead to roughly a net “+1” damage [4]. This has been found to be a reasonable approximation for modeling the extent of transient enhanced diffusion at higher temperatures. However, the validity of using a “+1” model for parameter extraction at lower temperatures is not clear [5]. Hence in this work we begin our simulations with the full damage cascade. Recent experiments of Cowern *et al.* [5] have shown that at low

temperatures small interstitial clusters are the main source of interstitials. For modeling interstitial clusters, we use the interstitial model derived by Cowern *et al.* [5]. This model was found to give good match to the experimental results using a “+1” approach. A model from previous work [6] is used for modeling the evolution of vacancy clusters. This vacancy cluster model was found to predict the results of gold decoration experiments [7] subsequent to annealing of high energy implants. As seen in Fig. 1, using the full damage leads to a good match to the experimental data of Cowern *et al.* [5]. It can be noted that the initial supersaturation is dominated by small interstitial clusters that ripen into larger {311} defects, thus dropping the supersaturation. Also shown in Fig. 1 is comparison of supersaturations using the full initial cascade to using a “+1” approximation. Both models were found to yield almost identical supersaturations. However looking at the total number of vacancies and interstitials in clusters, it can be noted (Fig. 2) that the recombination process is not complete and significant vacancy clusters are present until around 600 sec. This does not affect the supersaturation as it is governed by the small interstitial clusters. This also confirms the validity of using a “+1” model for lower temperatures where recombination may not have been completed.

B. Boron Interstitial Clusters

For modeling boron deactivation, we consider the clusters B_1I , B_2I_2 , B_2I , B_3I [1]. The reactions rates for each of these cluster interactions are included in PMM/DOPDEES, a system for solving PDEs in 1-D [8]. Clustering involves boron deactivation and formation of clusters of different charges. Hence it is necessary to include cluster charge states to be physically consistent. Based on charged defect calculations, Lenosky *et al.* [9] conclude that the dominant charge states for these clusters are $(B_1I)^+$, $(B_2I_2)^0$, $(B_2I)^0$ and $(B_3I)^-$. However, since electrical activation data indicates dominant clusters are neutral at room temperature, we assume the dominant cluster B_3I to be neutral $(B_3I)^0$. Reaction rates thus include interactions with all possible charged defect species. For example, the formation of $(B_1I)^+$ from mobile B_i and free I , can proceed by the following reactions:



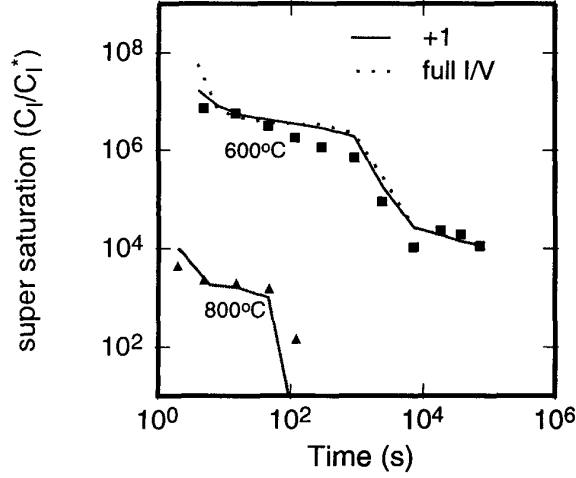


Fig. 1. Interstitial supersaturations at 600°C and 800°C obtained using full damage (bold lines) and using a “+1” model (dots) compared to data from Cowern *et al.* [5]. Note that the supersaturations obtained are almost independent of the initial conditions.

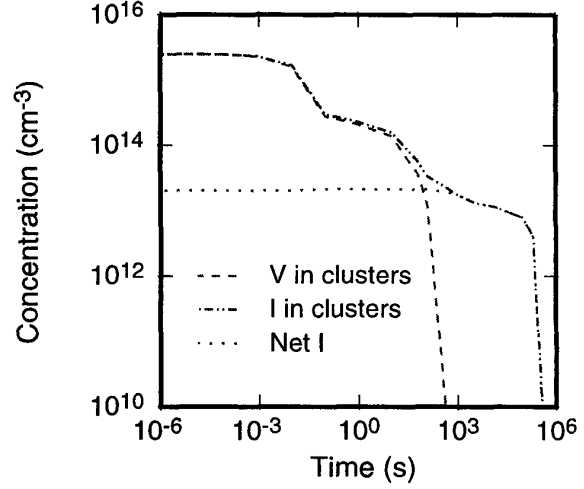
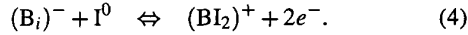
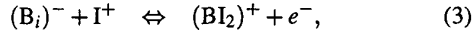
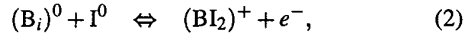


Fig. 2. Figure shows evolution of interstitial and vacancy clusters during annealing of a $2 \times 10^{13} \text{ cm}^{-2}$ Si implant at 600°C. The vacancies exist till around 600 sec, after which the interstitials trapped in interstitial clusters is close to a “+1”.



The overall net reaction rate is thus:

$$R_{BI_2} = k_{BI_2} \left[C_{(B_i)^0} C_{I^+} - \frac{C_{BI_2}}{K_{(B_i)^0/I^+}} \right], \quad (5)$$

$$k_{BI_2} = 4\pi a (D_{B_i} + D_I) \times \left(1 + \frac{1}{K_{I^+}} \frac{n}{n_i} \right) \left(1 + \frac{D_B^0}{D_B^+} \frac{n}{n_i} \right). \quad (6)$$

K_{I^+} accounts for the Fermi level dependence of interstitial concentration [10] and is defined such that:

$$C_I^+ = K_{I^+} C_I^0 \left(\frac{p}{n_i} \right). \quad (7)$$

Diffusivities of I and B_i are assumed to be independent of charge state.

III. RESULTS AND DISCUSSIONS

A temperature ramp-up of 50°C/s for the RTA and 1°C/s for the furnace anneals was used for the simulations. We compare our model to isochronal annealing results from Seidel *et al.* [11]. In these experiments, the active fraction of boron is measured as a function of temperature for a fixed

annealing time. Shown in Fig. 3 is a match to reverse annealing profiles from Seidel *et al.* [11] for two different implant doses. In these experiments boron was implanted at 150 keV and furnace annealed for 30 mins. At low temperatures (500 – 700°C, as shown in Fig. 3), boron clusters are stable and thus most of the boron is inactive. At higher temperatures (> 750°C), these boron clusters dissolve, and thus the active fraction increases as a function of temperature. Thus as shown in Fig. 3, our model captures the main features of the deactivation/activation process for different doses. This is also exhibited for higher doses, where the clustering behavior is stronger leading to lower activation.

We further compare our model to SRP and SIMS data from Pelaz *et al.* Fig. 4 shows the evolution of the active fraction compared to experimental data from Pelaz *et al.* [3]. Clusters form during the ramp-up to 800°C reducing the active fraction quickly. During further annealing, interstitial supersaturation drops rapidly subsequent to dissolution of interstitial defects. Thus this reduces the stability of boron interstitial clusters and leads to an increase in active boron fraction with time as shown in Fig. 4. Note that the dissolution process needs free interstitials for the formation of the intermediate species B_3I_2 , while dissolving from B_3I to B_2I . Thus activation of boron as seen in Fig. 4 is a slow process once these clusters are formed. Shown in Fig. 5 is comparison to a $2 \times 10^{14} \text{ cm}^{-2}$ B implant data from Pelaz *et al.* [3] spike annealed at 800°C. Similarly we find good match to experimental data for longer anneal times as shown in Fig. 6.

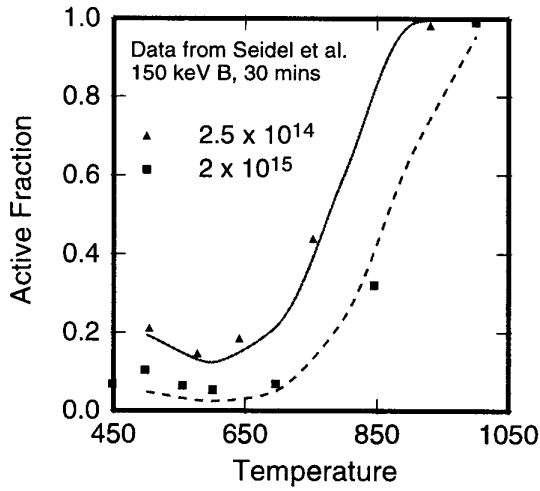


Fig. 3. Comparison of experimentally-measured active fraction [11] to model for 150 keV, $2 \times 10^{14} \text{ cm}^{-2}$ and $2 \times 10^{15} \text{ cm}^{-2}$ boron implants annealed for 30 min. at various temperatures. Lines represent model predictions, and symbols represent data.

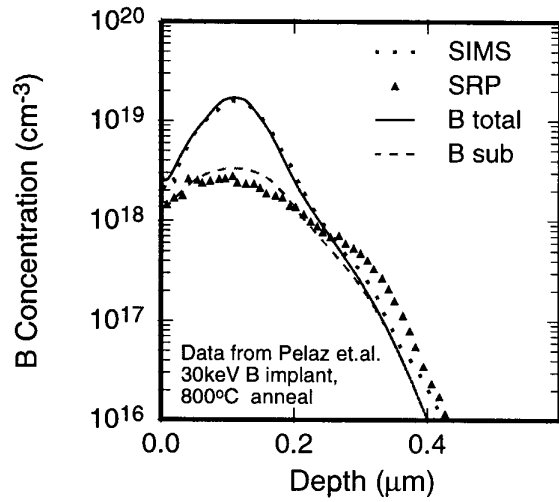


Fig. 5. Comparison of simulation with SIMS and SRP data from Pelaz *et al.* [3] for a $2 \times 10^{14} \text{ cm}^{-2}$ implant annealed at 800°C for 1 sec. Note that most of the boron is already in clusters.

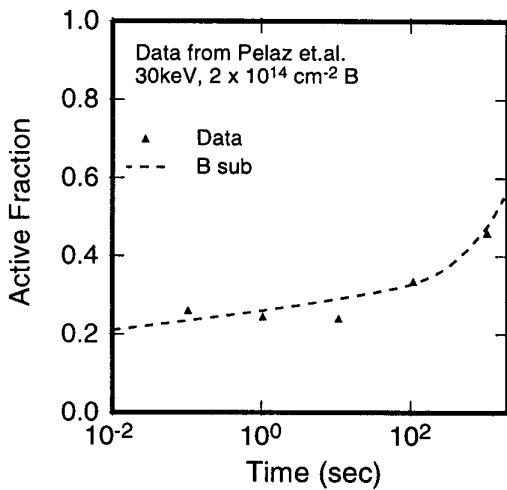


Fig. 4. Comparison of simulated and experimentally measured active fraction for a $2 \times 10^{14} \text{ cm}^{-2}$ boron implant annealed at 800°C. Data from Pelaz *et al.* [3].

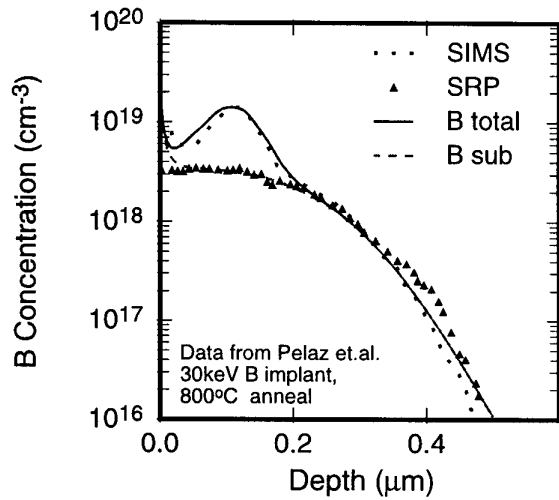


Fig. 6. Comparison of simulation with SIMS and SRP data from Pelaz *et al.* [3] for a $2 \times 10^{14} \text{ cm}^{-2}$ implant annealed at 800°C for 1000 sec.

IV. CONCLUSIONS

In summary, we have developed a boron clustering model to model boron deactivation kinetics during low and moderate temperature annealing after implantation. The model is able to capture the kinetics of the deactivation and activation processes and thus predict electrical activation during annealing over a wide range of temperatures and times.

ACKNOWLEDGEMENTS

We would like to thank Nick Cowern of Philips Research for details and discussions regarding their experimental results and model. This work was supported by the Semiconductor Research Corporation.

REFERENCES

- [1] S. Chakravarthi and S. T. Dunham, "A simple continuum model for simulation of boron interstitial clusters based on atomistic calculations," in *1998 International Conference on Simulation of Semiconductor Process and Devices, SISPAD'98 Technical Digest*, 1998.
- [2] M. J. Caturia, M. D. Johnson, and T. D. de la Rubia, "The fraction of substitutional boron in silicon during ion implantation and thermal annealing," *Appl. Phys. Lett.*, vol. 72, no. 21, pp. 2736, May 1998.
- [3] L. Pelaz, V.C. Venezia, H.-J. Gossmann, G.H. Gilmer, A.T. Fiory, C.S. Rafferty, M. Jaraiz, and J. Barbolla, "Activation and deactivation of implanted B in Si," *Appl. Phys. Lett.*, vol. 75, no. 24, pp. 662, Aug. 1999.
- [4] M.D. Giles, "Transient phosphorus diffusion below the amorphization threshold," *J. Electrochem. Soc.*, vol. 138, no. 4, pp. 1160, Apr. 1991.
- [5] N.E.B. Cowern, G. Mannino, P.A. Stolk, F. Roozeboom, H. G. A. Huizing, and J. G. M. van Berkum, "Energetics of self-interstitial clusters in Si," *Phys. Rev. Lett.*, vol. 82, no. 22, pp. 4460, May 1999.
- [6] S. Chakravarthi and S. T. Dunham, "Modeling of vacancy cluster formation in ion implanted silicon," in *Process Physics and Modeling in Semiconductor Technology*.
- [7] V. C. Venezia, D. J. Eaglesham, T. E. Haynes, A. Agarwal, D. C. Jacobson, H. J. Gossmann, and F. H. Baumann, "Depth profiling of vacancy clusters in MeV-implanted Si using Au labeling," *Appl. Phys. Lett.*, vol. 73, no. 20, pp. 2980, Nov. 1998.
- [8] A.H. Gencer and S.T. Dunham, "DOPDEES/PMM: A system for portable model description," in *Proceedings of the First International Conference on Modeling and Simulation of Microsystems, Semiconductors, Sensors and Actuators (MSM)*, Apr. 1998.
- [9] T. J. Lenosky, S. K. Theiss, and T.D. de la Rubia, "Private communication".
- [10] M.D. Giles, "Defect-coupled diffusion at high concentrations," *IEEE Trans. CAD*, vol. 8, pp. 460, 1989.
- [11] T.E. Seidel and A.U. MacRae, in *First Intl. Conf. on Ion Implantation*, F. Eisen and L. Chadderton, Eds., 1971, p. 149.